

Interfaces and the driving force of hydrophobic assembly

David Chandler¹

The hydrophobic effect — the tendency for oil and water to segregate — is important in diverse phenomena, from the cleaning of laundry, to the creation of micro-emulsions to make new materials, to the assembly of proteins into functional complexes. This effect is multifaceted depending on whether hydrophobic molecules are individually hydrated or driven to assemble into larger structures. Despite the basic principles underlying the hydrophobic effect being qualitatively well understood, only recently have theoretical developments begun to explain and quantify many features of this ubiquitous phenomenon.

Most general chemistry students are taught how detergent removes grease. An essential aspect of this process depends on the amphiphilic nature of the detergent molecules. Detergent molecules contain polar or charged components that happily interact with water (hydrophilic), and apolar components that by themselves do not easily dissolve in water (hydrophobic). Although these contrasting components would normally separate into a water-rich phase and an oil-rich phase, placing them next to each other in one molecule suppresses this macroscopic separation. Instead, the detergent molecules aggregate into mesoscopic fluid structures, such as micelles, with oily interiors and watery exteriors. Grease dissolves in aqueous detergent solutions by dispersing into the interiors of these aggregates. Similar effects influence more complicated assemblies¹, including biological structures where the separation of hydrophobic and hydrophilic components is a common feature².

In all these systems, an interaction mediated by water — the hydrophobic interaction — seems to cause clustering of hydrophobic units. This was noted by Walter Kauzmann in his influential 1959 paper³, and the idea is now widely accepted^{4,5}. But quantifying it in simple terms has been difficult because hydrophobicity is a multifaceted phenomenon that manifests different characteristics depending on whether small molecular units or large clusters are involved, or a combination of both. Here, I review these different regimes and theory to deal with them.

Contrasting length scales

The segregation of hydrophobic and hydrophilic phases or components results in a molecular interface that extends over distances (or 'lengths') that are large compared with the distances over which molecules affect one another in a homogeneous liquid. These interfaces distinguish mesoscopic structures, such as micelles, bilayers or microemulsions, from essentially nondescript intermolecular arrangements. For example, a few hydrated methane molecules and the alkyl groups of small alcohol molecules mixed with water show insignificant tendencies to cluster^{6,7}. Although the relative positions of small hydrophobic molecules in water are correlated, these correlation effects are modest and similar to what is seen for most small molecules in most homogeneous liquids. Such correlations in relative position are not a result of clustering, but arise from the effects of molecular size and shape^{8–11}.

The distances over which molecules influence one another in a homogeneous liquid typically approximate the girth of a molecule: about 0.3–0.5 nm for water or a small alkane. On this length scale, that is, the bulk liquid correlation length, molecular reorganization occurs readily because it involves only a modest thermodynamic cost. But reorganization to form an interface involves a significant cost. And if the interface is to remain, this cost or free energy of formation needs to be compensated for by forces that favour separation of the system into different phases. Because the interface cost grows linearly with surface area, whereas the compensating forces grow linearly with volume, a cluster can be stable or metastable only if it exceeds some critical size. This argument is familiar in the context of nucleation theory, which notes that a super-saturated solution will phase separate only after the formation of a critical nucleus¹². To be long-lived, hydrophobic clusters must extend over a minimum length (of 1 nm or more; see below).

Because bulk driving forces and interfacial costs compete, a consideration of only one of these quantities is generally insufficient to explain hydrophobic effects. And although efforts to infer hydrophobic interactions from molecular-scale surface areas alone are common^{13,14}, experimental observations illustrate the limitations of this approach. For example, the free energy required to transfer small hydrophobic molecules from oil to water differs by a factor of three compared with that inferred from interfacial cost considerations¹⁵. Moreover, while interfacial costs decrease with increasing temperature, hydrophobic forces show the opposite trend³.

Because hydrophobic interactions increase in strength with increasing temperature, they are often viewed as entropic; that is, hydrophobic units induce some order in the surrounding water. This idea is correct in as much as small hydrophobic units reduce the volume of configuration space available for hydrogen bonding. But the extreme view that pictures hydrophobic solvation in terms of rigid clathrate structures, like those surrounding hydrophobic particles in gas hydrates, is clearly incorrect: intermolecular correlations in liquid matter are insufficiently strong to be consistent with this crystalline picture. And while remnants of clathrate structure persist in the liquid near a small hydrophobic particle¹⁶, a surrounding clathrate structure is geometrically implausible in the case of extended hydrophobic surfaces.

¹Department of Chemistry, University of California, Berkeley, California 94720, USA.

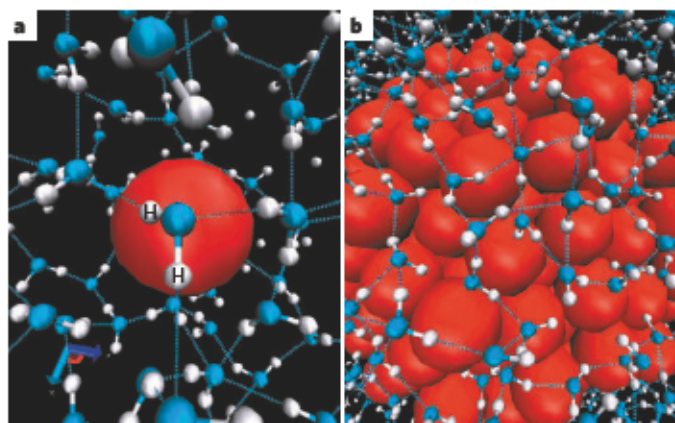


Figure 1 | Configurations of liquid water molecules near hydrophobic cavities in molecular-dynamics simulations. The blue and white particles represent the oxygen (O) and hydrogen (H) atoms, respectively, of the water molecules. The dashed lines indicate hydrogen bonds (that is, O–H...O within 35° of being linear and O-to-O bonds of no more than 0.35 nm in length). The space-filling size of the hydrophobic (red) particle in **a** is similar to that of a methane molecule. The hydrophobic cluster in **b** contains 135 methane-like particles that are hexagonally close-packed to form a roughly spherical unit of radius larger than 1 nm. In both cases, the water molecules shown are those that are within 0.8 nm of at least one methane-like particle. For the single cavity pictured in **a**, each water molecule can readily participate in four hydrogen bonds. (Owing to thermal motions, hydrogen bonding in liquid water is disordered.) Water molecules in **a** are typical of the bulk liquid where most molecules participate in four hydrogen bonds. The water molecules shown in **b**, however, are not typical of the bulk. Here, the cluster is sufficiently large that hydrogen bonds cannot simply go around the hydrophobic region. In this case, water molecules near the hydrophobic cluster have typically three or fewer hydrogen bonds.

Hydration of small and large cavities

Figure 1 illustrates this point by juxtaposing pictures of the hydration of small and large hydrophobic solutes. Most molecules dissolved in water have complicated shapes. Nevertheless, idealized spherical apolar particles or nearly spherical clusters, as pictured here, capture the most important physical features responsible for hydrophobic effects: acting like cavities in the water, these solutes exclude water molecules from the volumes they occupy, and they present regions of space where hydrogen bonding cannot occur.

Hydrophobic molecules interact with water in a variety of ways in addition to excluding volume. They exert weak attractive forces on water molecules by means of van der Waals interactions. They also exert strong attractive forces via hydrophilic components, such as the hydroxyl group on an alcohol. Although van der Waals interactions are too weak to affect the existence of interfaces in water, they do affect the position of an interface. Similarly, whereas hydrophilic parts of amphiphilic molecules are not directly responsible for hydrophobic assemblies, they do affect the arrangement of these assemblies relative to interfaces and other structures. We will look at both these effects, but first consider the most important physical features of hydrophobic solutes, all of which are found in the analysis of how cavities are solvated in water.

The small-solute case depicted in Fig. 1a illustrates the solvation of the cavity associated with a molecule such as methane. Namely, it excludes the centres of water molecules from a spherical volume less than 0.5 nm across. This volume is small enough that its presence in water requires no breaking of hydrogen bonds. Water molecules can adopt orientations that allow hydrogen-bonding patterns to go around the solute, and the extent to which bonds are broken at any instant is similar to that in the pure liquid. The situation is different in the large-solute case illustrated in Fig. 1b. Here, the solute surface extends with low curvature over areas larger than 1 nm², making it impossible for adjacent water molecules to maintain a complete hydrogen-bonding

network with the surrounding liquid. A fraction of the hydrogen-bonding possibilities are thus lost near an extended hydrophobic surface. To minimize the loss, on average, less than one hydrogen bond per water molecule is sacrificed compared with that in the bulk liquid. As a result, water tends to move away from the large solute and forms an interface around it akin to that between liquid and vapour.

This idea — that hydrogen bonding is maintained near a small hydrophobic region and not maintained near a large hydrophobic region — was expressed more than 30 years ago by Frank Stillinger¹⁷. It provides the physical basis for understanding hydrophobic effects.

Thermodynamics

Thermodynamic costs indicate whether processes are likely to occur and are conveniently quantified in terms of a free energy ΔG . In the context of solvating a molecule, ΔG is the reversible work for the solvent to reorganize and solvate the solute. The probability of solvation happening is proportional to $\exp(-\Delta G/k_B T)$, where T is temperature and k_B is Boltzmann's constant. This principle of statistical mechanics¹¹, which relates reversible work to probability, allows ΔG to be determined by measuring equilibrium constants, such as the concentration of the solute in water relative to that in some other environment. The free energy ΔG can also be computed using microscopic theory (see Box 1).

The free energy has two primary components: $\Delta G = \Delta H - T\Delta S$, where ΔH and ΔS are the enthalpic and entropic changes incurred during solvation. The enthalpic part is a measure of the average potential energy of interaction between molecules, and the entropic part is a measure of the order or intermolecular correlations¹⁸. The free energy of a process involving significant changes in the number of molecular interactions, such as the breaking of hydrogen bonds to form a liquid–vapour interface, will be dominated by its enthalpic component. In such cases, $\Delta G/T$ will decrease with increasing temperature.

A process that requires specific spatial organization of hydrogen-bonding patterns will have an important entropic component. At room temperature, for instance, the entropic cost of hydrating small hydrophobic species is dominant, as manifested by ΔG increasing with increasing temperature. With a sufficient increase in temperature, however, the extent of hydrogen bonding between water molecules diminishes, and maintaining hydrogen bonds becomes less important. In fact, whereas the entropy change associated with the hydration of a

Box 1 | Calculating solvation energies

Dissolving a substance in a solvent can be regarded as transforming a system from state 1 (pure solvent) to state 2 (solvent plus solute). This process is associated with a change in free energy, $\Delta G = G_2 - G_1$, which in our example is the solvation free energy. Macroscopic properties such as ΔG can be determined from the molecular properties and molecular interactions of the system (captured through so-called partition functions Z) using statistical thermodynamics¹¹:

$$\Delta G = G_2 - G_1 = -k_B T \ln(Z_2/Z_1) \quad (1)$$

$$= -k_B T \ln(\langle \exp(-\Delta E/k_B T) \rangle_1) \quad (2)$$

$$= \langle \Delta E \rangle_1 \quad (3)$$

Here, ΔE denotes the difference in microstate energy between states 2 and 1, and $\langle \dots \rangle_1$ denotes the equilibrium ensemble average (that is, the Boltzmann-weighted average) over the microstates of state 1. The third approximate equality is valid when $\Delta E/k_B T$ is predominantly small in the ensemble of microstates. The averages in equations (2) and (3) can be computed in a number of ways⁵⁹ to obtain ΔG .

A 'Boltzmann weight' of a microstate is the exponential of the energy in units of $-k_B T$. Thus, this thermal energy $k_B T$ is the energy scale of statistical thermodynamics against which energies or free energies are described as 'small' or 'large'. Microstates with small energy differences have similar probabilities and the more such states near a given energy, the larger the entropy. A partition function for a specific macroscopically controlled state is the Boltzmann-weighted sum over all microstates consistent with that control. The entropic contribution to free energy comes from the number of terms in that sum available at a given energy.

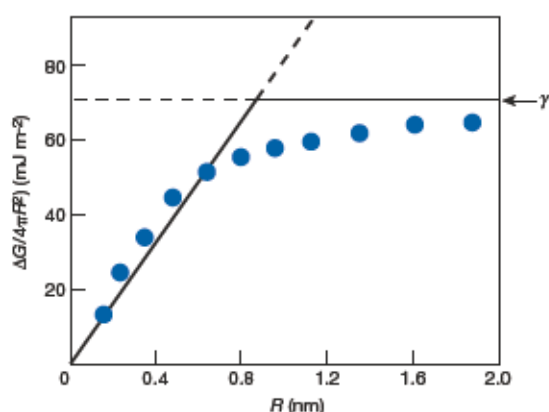


Figure 2 | Solvation free energy, ΔG , for a spherical cavity in water as a function of the cavity size. The results are for ambient conditions (room temperature and 1 atm pressure). The circles show the results of detailed microscopic calculations²⁵. The liquid–vapour surface tension is shown by γ . The solid lines show the approximate scaling behaviour of $\Delta G/4\pi R^2$ for small R , and the asymptotic behaviour for large R . This approach can be used to infer the typical length characterizing the crossover behaviour, but not the quantitative behaviour of ΔG in the crossover regime.

Box 2 | Free energy for small cavities in water

For a cavity with volume v (which need not be spherical), the difference in microstate energy ΔE is infinite whenever a solvent particle is in the cavity, and zero otherwise. This implies that the solvation energy ΔG_v of the cavity depends on $P_v(N)$, the probability of finding in a volume v of pure solvent, N solvent molecules. According to equation (2) from Box 1, $\Delta G_v = -k_B T \ln P_v(0)$. For small volumes, the probability $P_v(N)$ is almost exactly gaussian⁵⁰, and ΔG_v can therefore be expressed analytically in terms of the cavity volume v , the mean number of molecules that occupy that volume in the pure liquid $\langle N \rangle_v = v\rho$, where ρ is solvent density, and the mean-square fluctuation in that number of molecules χ_v . In particular we find that⁵⁰:

$$\Delta G \approx k_B T \rho^2 v^2 / 2\chi_v + k_B T (\ln 2\pi\chi_v) / 2 \quad (4)$$

with

$$\chi_v = \langle (\delta N)^2 \rangle_v = \rho v + \rho^2 \int_v \int_v d\mathbf{r} d\mathbf{r}' [g(|\mathbf{r} - \mathbf{r}'|) - 1] \quad (5)$$

The integrand for integrals over the cavity volumes in the second equality in equation (5) is the pair correlation function for the pure liquid. Given that the radial distribution function, $g(r)$, is unity beyond the correlation length of the liquid, it follows that χ_v is roughly proportional to v . This behaviour together with equation (4) explains why ΔG for small hydrophobic solutes is approximately linear in solute volume.

The temperature dependence obtained from equation (4) approximates the temperature dependence of ΔG for small hydrophobic molecules in water⁵⁰. For example, consider a cavity of diameter 0.35 nm, as would be appropriate for methane. The entropy of solvation, $\Delta S = -\partial \Delta G / \partial T$, calculated from equation (4) at room temperature, is 20 cal mol⁻¹ K⁻¹. The heat capacity of solvation, $\Delta C_p = -T \partial^2 \Delta G / \partial T^2$, computed from equation (4) for that same cavity in water, is about 50 cal mol⁻¹ K⁻¹. These numbers agree well with those measured for methane in water at room temperature, about 17 cal mol⁻¹ K⁻¹ and 50 cal mol⁻¹ K⁻¹ for the solvation entropy⁶¹ and heat capacity⁶¹, respectively.

Equations (4) and (5), due to Pratt and his coworkers^{50,60}, can be applied easily to cavities and yield accurate solvation free energies for hydrophobic molecules of arbitrary shape, provided the molecules are not large. The older theory^{8,40} of hydrophobic solvation and interaction has similar generality, a similar range of applicability, and a similar, although less transparent, basis in gaussian statistics⁶². When this approach fails, the failure is due to the formation of interfaces, in which case a more general theory is applicable²⁰. These theories do not require the extent of microscopic detail that is considered important in some approaches^{63,64}. Once a cavity is specified, whether spherical or otherwise, all quantities entering into formulae for solvation free energies and solute distribution functions are experimentally measurable.

small alkane at room temperature is negative (and reasonably large in magnitude), it becomes positive near the boiling temperature of water¹⁹.

Interfaces and size scaling of ΔG

At ambient conditions (room temperature and 1 atm pressure), liquid water lies close to phase coexistence with its vapour; that is, the free-energy difference between water in its liquid and vapour phases is small compared with the thermal energy available for molecules to move from the liquid to the vapour phase. This condition ensures that large cavities in water are accompanied by an interface like that between liquid and vapour, as suggested by Stillinger¹⁷, and confirmed by theoretical analysis^{20,21} and simulation^{22–26}. The cost to hydrate the large spherical cavity of radius R is thus $\Delta G \approx 4\pi R^2 \gamma + (4/3)\pi R^3 p \approx 4\pi R^2 \gamma$, where γ refers to the liquid–vapour surface tension, and p to the pressure, both at the temperature considered. The pressure–volume term $(4/3)\pi R^3 p$ would be important for macroscopic cavities, but is negligible at standard pressures provided R is less than several nanometres.

Changing the thermodynamic state, so as to move away from liquid–vapour coexistence, reduces the tendency to form a liquid–vapour-like interface near large cavities. Furthermore, the demand for interface formation — to minimize the number of broken hydrogen bonds — is diminished at high pressures, high temperatures, or both because these conditions lead to high concentrations of broken hydrogen bonds, even in the absence of interfaces. At standard conditions, however, a large hydrophobic solute does induce the surrounding water to form an interface, so that its solvation free energy contains a component that is proportional to surface area.

In contrast, the hydration of a small solute does not lead to broken hydrogen bonds, but involves a re-ordering of hydrogen bonds. This re-ordering persists into the surrounding liquid for a distance of about one correlation length (see also Box 2). Because correlations in water extend over the girth of a typical small molecule, adding up the points over which a small solute will affect correlations in water gives a solvation free energy that scales more like the volume than like the surface area of the solute. The ΔG needed to hydrate a small sphere will thus scale more accurately as R^3 than as R^2 (Box 2).

Figure 2 illustrates how solvation free energy (normalized to surface area) changes with solute size, and how the different trends for small and large hydrophobic solutes change once a radius of about 1 nm is reached. For smaller solutes, the solvation free energy grows linearly with solute volume; for larger solutes, it grows linearly with surface area. The crossover behaviour arises because only larger solutes induce adjacent water to form an interface. However, this crossover phenomenon is not a phase transition where collective motion on a macroscopic scale results in sudden or singular changes. The crossover pertinent to hydrophobicity is collective, but it occurs on a microscopic scale where nothing so precipitous as a true transition can occur.

Hydrophobic molecules: wet or dry?

The behaviour of water near hydrophobic solutes can be probed in detail by microscopic calculations, which average behaviour over microstates of the solvent in the presence (or absence) of the solute (see also Box 1). For example, Fig. 3 shows the density of solvent, relative to that of the bulk solvent, near a series of hydrophobic solute models of different sizes. For the cavity with the smallest excluded volume radius, $R = 0.4$ nm, the water density immediately adjacent to the solute surface is increased by a factor of two. In this case, the solute is said to be ‘wet’. The significant increase in water density adjacent to this cavity results from the liquid responding elastically to the cavity: water molecules are localized so as to maintain hydrogen bonding. In contrast, the larger cavities with $R = 1, 10$ and 100 nm are ‘dewetted’ or ‘dry’ because the large cavity has caused the source of elasticity — the hydrogen bond network — to break, so that the liquid moves away. The similarity between the interfaces formed here

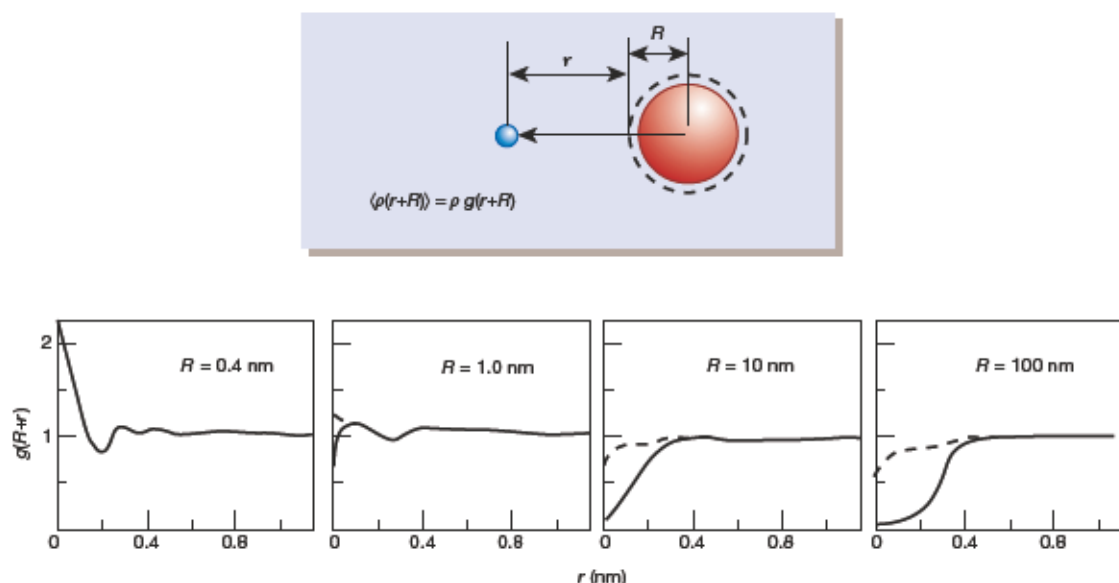


Figure 3 | The average equilibrium density of water a distance $r + R$ from spherical cavities in liquid water at standard conditions. R is the distance of closest approach between the centre of a water molecule (red circle) and the centre of the cavity (blue circle). The lines representing $g(r + R)$, the density, $\langle \rho(r + R) \rangle$ relative to that of the bulk water, ρ , are the results of microscopic theory^{21,24}. Solid lines refer to the ideal hydrophobic

solute, which expels water from the sphere of radius R . Dashed lines refer to the case where the cavity also interacts with water by means of a van der Waals attraction typical of that between water and a spherical cluster of oil. For cavities with radii less than 1 nm, the effects of this attraction on $g(r + R)$ are nearly negligible and not visible on the scale of the graph in the bottom panel.

and the liquid–vapour interface is especially clear for the largest of these cavities.

In formal statistical mechanical parlance, a wet surface is a surface covered by a macroscopically thick liquid layer or film, whereas a dry surface is covered by a macroscopically thick vapour layer. Capillary condensation is an example of wetting in this formal sense²⁷. In contrast, my use of these terms in this review refers to microscopic phenomena, and is descriptive rather than formal. In fact, van der Waals attraction between surface and solvent ensures that no natural macroscopic hydrophobic surface can be dry in the formal sense: the free-energy cost needed to move the liquid macroscopically far from the surface would be prohibitive. Nevertheless, compared with the density of water surrounding a small hydrophobic molecule or a hydrophilic surface, nanometre-sized and larger hydrophobic surfaces in water are indeed dewetted in the descriptive sense.

Experimental measures of the solvation free energy ΔG come from the free-energy change that occurs on transferring a hydrophobic molecule from its pure liquid to liquid water. For *n*-alkanes with 20 or fewer carbon atoms, the transfer free energy is a linear function of carbon number²⁸. Because the volume of a chain-like molecule grows linearly with the number of units, the linear trend in transfer free energies with carbon number is consistent with ΔG growing linearly with cavity volume, as expected for a small wet solute. However, the length of a 20-carbon alkane chain in coil conformation typically exceeds 1 nm, the crossover length beyond which large-solute solvation is expected. Because the curvatures of these hydrophobic surfaces are sufficiently high, they can still be hydrated as in the small-molecule regime. Globular conformations would present an extended hydrophobic surface with lower curvature that would prevent this type of hydration: if prevalent, these globular conformations would therefore lead to a change in the transfer free-energy trend. The fact that this trend remains linear for *n*-alkanes with 20, or fewer, carbons indicates that these molecules are rarely globular. In other words, with this number of carbons, hydrophobic forces seem to be insufficient to overwhelm chain entropy and stiffness that favour the coil state.

Driving force of assembly

The tendency for hydrophobic particles to cluster in water is readily understood in terms of the dependence of hydrophobic solvation on solute size. For example, imagine n identical small hydrophobic particles solvated in water, all well separated and thus solvated independently of each other. In this case, the overall solvation free energy is n times the solvation free energy for any one of the solutes, and it grows linearly with the overall excluded volume of the solutes.

When these n solutes cluster together to form a hydrophobic unit with an extended surface (that is, a surface with low curvature and larger than 1 nm²), the overall solvation free energy changes from growing linearly with solvated volume to growing linearly with solvated surface area. Figure 4 illustrates that if n is large enough, the solutes can form a cluster with a sufficiently large volume to surface ratio that its solvation free energy is lower than the overall solvation free energy of the individual solutes. This effect results in a favourable driving force for cluster assembly. The figure also illustrates that near ambient conditions, the driving force will get stronger with increasing T . This well-known trend is often cited as implying that hydrophobic interactions are entropic²⁹. Entropy does indeed contribute, but the assembly process is driven by the difference between the entropically dominated solvation free energy of small molecules and the enthalpically dominated solvation free energy of large surfaces.

A hydrophobic force that drives cluster assembly will be proportional to the change in solvated hydrophobic surface area only if all surfaces are sufficiently large. Generally, this is not the case. For example, when a collection of small hydrophobic units assembles into an extended cluster, such as that depicted in Fig. 4, the force driving the process will consist of one part that is proportional to the exposed surface area of the cluster, and another part that is proportional to the molecular volumes of the separate units. In physical situations such as this, with small as well as large length-scale regimes having a role, hydrophobic forces cease to be additive. Although hydrophobic forces between isolated small hydrophobic units can be decomposed into pair interactions, this is no longer possible as the units combine to form an extended hydrophobic surface and an associated solvent interface. This breakdown in additivity of hydrophobic forces is a manifest-

tation of the collective nature of interface formation.

At extremely low hydrophobic solute concentrations, the entropy of mixing solute molecules throughout a macroscopic container (which gives an effectively infinite volume) overwhelms the finite driving force to assemble, making clusters of finite size no more than metastable. On the other hand, finite solvent volumes will give rise to modest solute densities, and thus modest entropies of mixing, which need not defeat finite driving forces for hydrophobic association of the solutes. A computer simulation using such a finite solvent volume confirms that stable association requires hydrophobic clusters that extend beyond a critical radius of about 1 nm (ref. 30).

When hydrophobic particles are connected in a chain, the entropy favouring the extended state is finite, even in a system with infinite volume. Hydrophobic collapse in such a situation, with the chain going from a coil to a globule, involves transition states that coincide with the formation of critical nuclei of hydrophobic particles³¹; subsequent motions are committed to the stable globular conformations. The critical nuclei are formed in many ways, but always lead to the formation of a liquid–vapour-like interface. This interface then allows for fluctuations in water density, and these fluctuations permit the solvated chain to progress towards its stable globular state where the chain's interior is dry. Intriguingly, these solvent fluctuations, rather than chain dynamics, dominate the motion of the system through the transition states. The correct treatment of the hydrophobic collapse kinetics must therefore explicitly account for water dynamics, which precludes using solvent averaged potentials of mean force.

Role of weak attractive forces

Weak attractive forces, such as van der Waals interactions, are generally assumed to have little or no influence on the structure of a dense fluid³²: because density is high, the liquid is almost incompressible, eliminating all but small-length-scale density fluctuations. Instead, liquid structure is thought to be influenced only by packing effects, and by strong attractions that vary quickly in space, such as hydrogen bonds. This idea is a useful starting point for thinking about dense fluids. But it is not entirely applicable in the context of hydrophobicity, which involves interfaces forming in water near an extended hydrophobic surface.

Extended fluid interfaces near or at phase coexistence are often referred to as 'soft' because they can be translated in space with little or

Box 3 | Solvation effects of van der Waals interactions

In the case of small solutes, van der Waals attractions have little influence on the surrounding water structure (see also Fig. 3). Their contribution to the overall solvation free energy ΔG can therefore be estimated according to¹¹

$$\Delta G = \Delta G_v + \rho \int dr g_v(r) u(r) \quad (6)$$

where ρ is the solute density, $g_v(r)$ the relative average density of solvent in the presence and absence of the solute cavity, and $u(r)$ the added van der Waals potential acting on the solvent at position r . The integral in equation (6) is approximately linear in volume for small solutes, as is ΔG_v . The accuracy of equation (6) in estimating van der Waals contributions to solvation free energy has been verified by comparison against computer simulations⁶⁵.

The van der Waals contribution affects the overall solvation free energy ΔG appreciably, but its influence on the entropy of solvation ΔS ($= -\partial G/\partial T$) is rather subtle, mediated only through the temperature dependence of the cavity–water distribution function $g_v(r)$. This justifies using a cavity model to estimate hydrophobic solvation entropies and heat capacities^{50,52}.

Van der Waals interactions are attractive, so $u(r)$ is negative and contributes to ΔG such that it favours solvation. This contribution is primarily enthalpic, whereas ΔG_v itself is primarily entropic.

In the case of large hydrophobic solutes interacting through van der Waals forces with surrounding water, the average water density is well approximated as the bulk density at all points not occupied by the solute (see also Fig. 3). That is, $g_v(r)$ in equation (6) can be approximated by unity for all r outside the solute, and by zero otherwise. The integral then gives a favourable enthalpic contribution to ΔG , but scales linearly with solute surface area rather than with solute volume. For large solutes, therefore, size scaling and trends with temperature are the same for both the cavity and the van der Waals contributions to ΔG .

no free-energy change¹. As a result of this softness, the location of the liquid–vapour-like interface, and the average liquid density near a large hydrophobic surface, can be significantly affected by van der Waals attractions. As illustrated in Fig. 3, for the case of a small hydrophobic solute where a soft interface does not accompany solvation, adding typical oil–water van der Waals attractions has essentially no effect on the average density of the surrounding water. But in the case of larger solutes that are accompanied by a soft interface, adding weak attractive forces brings the liquid interface into contact with the hydrophobic surface.

The resultant close proximity of the liquid interface to the hydrophobic surface and the larger average value of the liquid density near that surface has caused some to overlook dewetting, imagining the surface to be wet instead²⁴. A wet surface, however, is markedly different: although interfacial displacements and thus density fluctuations are substantial for water at its liquid–vapour interface and for water near an extended hydrophobic surface, they are largely absent for water adjacent to a wet surface. As a result of weak, but ubiquitous, attractive forces between oil and water, the main signature of dewetting is thus not the mean water density near the hydrophobic surface but the size of spontaneous density fluctuations. These fluctuations determine the degree to which weak attractions can affect the mean water density, even though the specific value of the mean for a particular choice of attraction has little physical significance. In contrast, the likelihood of fluctuations has an important role in the kinetics of hydrophobic assembly³¹.

Experiments confirm that the oil–water interface is much like the liquid–vapour interface of water, with no significant excess water density relative to the bulk water^{33–36}. In fact, the water–oil surface tension can be accurately approximated as the liquid–vapour surface tension plus the negative contribution arising from oil–water van der Waals interactions (see also Box 3). This readily explains why the tension of the oil–water interface is 20% lower than the surface tension of water²¹.

Similarly, the effect of van der Waals attractions on the solvation energies of small hydrophobic molecules can be readily computed, given

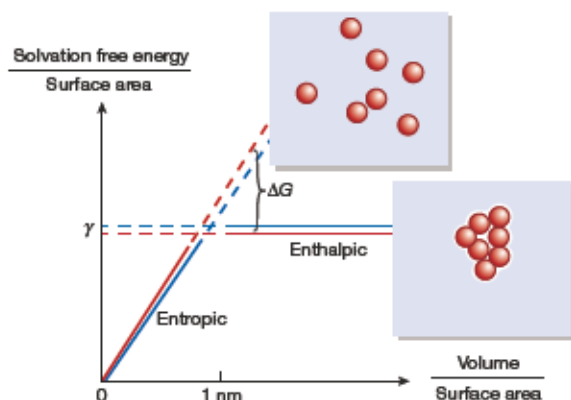


Figure 4 | The driving force, ΔG , for assembling a cluster of small hydrophobic particles. For large enough clusters, ΔG is a favourable driving force. The horizontal and sloping lines indicate the behaviour of the solvation free energy for the assembled and disassembled cluster, respectively. Red lines indicate the free energies at a higher liquid temperature; blue lines indicate the free energies at a lower temperature. The liquid–vapour surface tension is indicated by γ . 'Volume' and 'surface area' denote the volume excluded to water, and the solvated surface area of that volume, respectively.

that these attractions have no appreciable effect on average solvent density (Box 3). This fact is codified in equation (6) in Box 3. Theory accounting for these attractions can also explain why methane, ethane and propane all have similar solvation free energies, an observation that is often incorrectly perceived as puzzling and incompatible with our understanding of hydrophobic interactions (see Box 4). Finally, because scaling with respect to solute size is not affected by van der Waals interactions in either the small-molecule or large-surface regime, it is straightforward to anticipate the effects of these interactions on the crossover length and on the thermodynamic driving force for clustering.

Strong attractive forces and amphiphile assembly

The effects of strong attractions between water and hydrophilic units differ from the effects of weak interactions, in that strong attractions tend to localize water molecules to specific locations and thereby limit fluctuations. This effect is important for the self-assembly in water of amphiphilic molecules, which contain hydrophobic as well as hydrophilic components. Such solutions form an array of mesoscopic assemblies that are at least partly stabilized by hydrophobic forces^{1,29,37}.

Box 4 | The small alkane solubility 'paradox'

In water at standard conditions, the solvation free energies of methane (CH_4), ethane ($\text{CH}_3\text{-CH}_3$), and propane ($\text{CH}_3\text{-CH}_2\text{-CH}_3$) are all about the same, differing by no more than 10% from 2 kcal mol^{-1} (ref. 66). This similarity, often perceived as perplexing, is readily explained.

Consider first methane. Its solvation free energy ΔG_{Me} accounts for the formation of the methane cavity, $\Delta G_{\text{Me}}^{(0)}$, and for van der Waals attraction between methane and water, $-\epsilon$. We assume that methane forms a spherical cavity in water with $R \approx 0.35 \text{ nm}$, and use equation (4) from Box 2 to estimate $\Delta G_{\text{Me}}^{(0)} \approx 7 \text{ kcal mol}^{-1}$. From $\Delta G_{\text{Me}} = \Delta G_{\text{Me}}^{(0)} - \epsilon$, and the experimental value of ΔG_{Me} of about 2 kcal mol^{-1} , we obtain $\epsilon \approx 5 \text{ kcal mol}^{-1}$.

The solvation free energy of ethane ΔG_{Et} might be estimated relative to that of two methane molecules, given that the solvation of an ethane molecule should be nearly identical to that of two overlapping methane particles⁶⁷. (The idea of two undistorted methane molecules occurring in such close proximity is unrealistic, but it is only the appearance of the solute to the solvent that determines the solvation free energy.) Thus $\Delta G_{\text{Et}} \approx 2\Delta G_{\text{Me}} + \Delta w(L)$, where $\Delta w(L)$ is the reversible work to bring two methane cavities in water to a separation L (equal to the C-C bond length in ethane). The reversible work must account for the difference in solvation free energies for cavities at infinite separation ∞ and at separation L , $\Delta G_{\text{v}(L)} - \Delta G_{\text{v}(\infty)}$, and for attractive methane-methane interactions, $u_{\text{MeMe}}(L)$. (The latter must be added to the cavity-cavity potential of mean force to account for the fact that the full radial distribution function is well approximated by the cavity radial distribution function³².) For water at standard conditions, the result is $\Delta w(L) = \Delta G_{\text{v}(L)} - \Delta G_{\text{v}(\infty)} + u_{\text{MeMe}}(L) \approx -2 \text{ kcal mol}^{-1}$. Together with the methane solvation free energy ΔG_{Me} , this yields an ethane solvation free energy $\Delta G_{\text{Et}} \approx 2 \text{ kcal mol}^{-1}$.

Similarly, the solvation free energy of propane ΔG_{Pr} might be estimated by considering separated cavities for methane and ethane in water that are reversibly moved together, so as to form a propane cavity. As this can be done roughly collinearly, the reversible work required to achieve this should be about the same as that needed for joining two methane cavities: $\Delta G_{\text{Pr}} \approx \Delta G_{\text{Et}} + \Delta G_{\text{Me}} + \Delta w(L)$. Again, $\Delta w(L)$ approximately cancels ΔG_{Me} , so ΔG_{Pr} has a value similar to ΔG_{Et} and ΔG_{Me} . Similar arguments can be used to estimate solvation free energies of short cyclo-alkanes in water relative to those of the corresponding normal alkane, indicating that $\Delta G_{\text{cyclo}} \approx \Delta G_{\text{normal}} + \Delta w(L)$. Experiment⁶⁸ confirms that the former is indeed between 1–2 kcal mol^{-1} less than the latter.

The fact that $\Delta w(L)$ is close to $-\Delta G_{\text{Me}}$ is a coincidence, true for water at standard conditions but not true in general. Somewhat different values for the van der Waals attraction ϵ and the mean water density fluctuation χ_w would not change the basic physics, but would void the near cancellation that results in similar solvation free energies for methane, ethane and propane. The argument sketched here does, however, result in the generally valid prediction that the solvation free energy of a small normal alkane chain should scale linearly with the number of carbons, with a slope $\Delta G_{\text{Me}} + w(L)$. The scaling is found experimentally for the free energy to transfer an alkane chain from oil to water^{28,29}, with the cavity model yielding an estimate^{8,9} of the difference between $\Delta G_{\text{Me}} + w(L)$ for oil and for water that agrees well with the experimental slope.

The principles that hold for purely hydrophobic solutes also apply to molecules containing some hydrophilic units. But additional entropic effects arise because molecular configurations are restricted when both hydrophilic and hydrophobic interactions need to be accommodated. This is illustrated in the simplest example of amphiphilic assembly — micelle formation (see Fig. 5).

The free energy for solvating an amphiphile either in water or in a micelle with an oily interior can be approximated by considering the free-energy contributions of its hydrophilic head and hydrophobic tail separately. The hydrophilic head will always be in an aqueous environment, so the free energy for transferring an amphiphile from a micelle into water, g_{trans} , approximately equals the free energy for transferring the corresponding hydrophobic molecule from oil to water. The force driving the assembly of a micelle with n amphiphilic molecules, ΔG_n , will therefore contain the contribution $-ng_{\text{trans}}$. This contribution favours the formation of a micelle, but is opposed by two other free-energy contributions. One arises from the fact that the formation of a micelle involves the creation of an interface, as is familiar from nucleation theory¹². A second opposing contribution is entropic. This accounts for the reduction in configurations available to amphiphilic molecules when hydrophobic chains are constrained to lie within a micelle while the head groups are confined to the micelle surface. This effect limits micelle growth to a finite size: for large n , there is simply no space available to maintain a dense micelle interior while simultaneously placing head groups on the exterior.

Given these different free-energy contributions, the principle of association equilibrium¹¹ (that is, the law of mass action) readily explains³⁸ why the critical micelle concentration decreases exponentially with amphiphile chain length, and further why this concentration decreases with increasing T at low T , but increases with T at high T . The exponential behaviour with chain length reflects the linearity of oil-water transfer free energy as a function of hydrophobic molecule chain length²⁹. The non-monotonic trend with temperature reflects the fact that transfer free energies are similarly non-monotonic (that is, ΔS for hydrophobic solvation passes through zero at a convergence temperature).

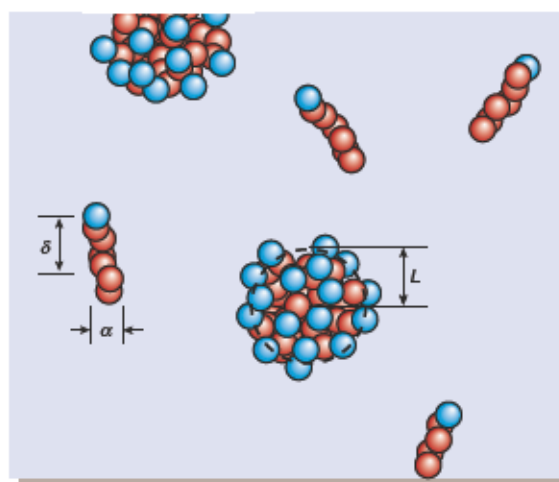


Figure 5 | Lengths scales of amphiphiles in dynamic equilibrium with micelles. The blue and red spheres depict the hydrophilic heads and the hydrophobic tails, respectively, of the amphiphiles. The typical length over which hydrophobic and hydrophilic components are separated within a single molecule is given by δ . Assuming a roughly spherical structure and tightly packed oily components in the centre, the micelle radius is $L = (\alpha^2 \delta)^{1/3} n^{1/3}$, where n is the number of surfactants in the micelle. Accounting for the hydrophobic driving force for assembly, plus interfacial and entropic free-energy costs, the average size of the micelle is found to be $n = \beta \gamma \delta^2$ (where $\beta = 1/k_B T$ and γ is the oil-water surface tension), and the critical micelle concentration approximately $(1/\alpha^3) \exp[-\beta g_{\text{trans}} + c(\beta \gamma \alpha^2)^{2/3}]$, where g_{trans} is the oil-to-water transfer free energy for the oily chain of an amphiphile and $c = (5,832/49)^{1/3} \approx 4.9$ (ref. 38).

Is water special?

Much has been written on the question of whether water is special and about its importance in biology (for examples, see refs 39, 40). Considering its thermodynamic anomalies, patterns of hydrogen bonding, ability to support fast proton transport and so forth, liquid water is obviously a unique solvent. Nevertheless, the two physical features responsible for hydrophobicity — the solvent being close to phase coexistence with its vapour, and solute–solvent interactions being significantly less attractive than solvent–solvent interactions — are not particularly unusual, at least in an abstract sense.

The proximity of phase coexistence and the imbalance of attractive forces can be satisfied with model systems that have little in common with water. Their only similarity with water is a high molecular density at conditions of low pressure; that is, the solvent, like water, is close to its triple point. For example, a Lennard–Jones solvent^{41–43}, a two-dimensional fluid model⁴⁴ and even a two-state lattice gas^{45,46} all provide perfectly acceptable models that will show behaviour akin to hydrophobicity, including amphiphilic self assembly^{47–49}.

In nature, however, it is difficult to find a pairing of liquids that show an attractive force imbalance that is similar to that found for water and oil. This imbalance is due to hydrogen bonding between water molecules, and produces the crossover in solvation behaviour at a length scale of 1 nm and at thermodynamic conditions near 1 atm pressure and room temperature. Furthermore, the temperature dependence of the structure of water's hydrogen-bond network leads to the relatively large temperature dependence of solvation entropies described earlier. This temperature dependence of solvation entropies has a significant role in the temperature dependence of assembly processes (see Fig. 4), and is considered important in the context of protein folding^{50–53}.

To the future

It is one thing to understand the forces underlying hydrophobic interactions, but quite another to appreciate all the interesting implications such forces have. For example, a correct and useful theory of hydrophobic effects should provide quantitative guidance for the study of biophysical systems. Do we now have such a theory? Perhaps, but its usefulness remains to be demonstrated.

One area where progress might soon be made is the study of protein–protein interactions controlling self-assembly of large protein complexes. Here, challenges arise from the presence of two types of disorder⁵⁴: the fact that the hydrophobic surfaces of proteins are laced with hydrophilic units, and that the surfaces are irregular in shape. These features will affect the size of hydrophobic units, and hence how hydrophobic interactions arise, as well as their strengths and kinetics. For example, hydrophilic units will probably lessen the extent of drying and thereby allow water to lubricate the final stages of assembly in a protein complex⁵⁵. In addition, the exact placement of hydrophilic units and the specifics of surface topography should influence the complementarities of protein surfaces. Similar issues should also present important challenges when trying to elucidate the role of hydrophobic effects in intramolecular processes such as protein folding.

Materials science is another area where our understanding of hydrophobic effects might prove useful. For example, drying-mediated self-assembly of nanoparticles involves competition between the kinetics of evaporation and the time scales with which solvated nanoparticles diffuse on a substrate⁵⁶. How these effects might be enriched by surfaces that nucleate evaporation remains to be explored. Such systems, and also the adhesion between macroscopic surfaces, involve pertinent length scales other than just the crossover length (which is essentially the radius of a critical nucleus of oil in a super-saturated water–oil mixture). For example, the confinement of water by two macroscopic hydrophobic surfaces in solution can induce evaporation of the confined liquid because the oil–water interfacial free energy outweighs the free energy favouring liquid water over its vapour phase. For flat, parallel surfaces in water at standard conditions, the inter-surface separation exceeds 1,000 nm where evaporation becomes favourable.

Surface-induced evaporation of this sort between macroscopic

plates would produce a macroscopic adhesive force, but it requires that evaporation be kinetically accessible. This can occur through interfacial fluctuations that bring two separate interfaces in water into contact⁵⁷. In the case of hydrated mesoscopic hydrophobic surfaces, such fluctuations are feasible because the confined liquid remains stable until the surfaces are relatively close together. But for macroscopic surfaces, the free-energy cost for such fluctuations is prohibitive, and evaporation is possible only through other pathways. In particular, a liquid sufficiently confined by unfavourable surfaces will become mechanically unstable, causing, in effect, spinodal decomposition. For pure water, this instability is estimated²⁰ to occur when two macroscopic hydrophobic surfaces are separated by about 5 nm, which is similar to the separation at which forces become unstable for two hydrated hydrophobic surfaces in a surface–force apparatus⁵⁸.

Whether these specific phenomena prove significant, there is no doubt that the hydrophobic effect is fundamental. The varied and possible complexities of aqueous solutions where the hydrophobic effect is manifested provide ample opportunity to probe the underlying general principles outlined in this review. ■

1. Safran, S. A. *Statistical Thermodynamics of Surfaces, Interfaces and Membranes* Ch. 1–3 (Addison-Wesley, Reading, 1994).
2. Tanford, C. The hydrophobic effect and the organization of living matter. *Science* **200**, 1012–1018 (1978).
3. Kauzmann, W. Some forces in the interpretation of protein denaturation. *Adv. Prot. Chem.* **14**, 1–63 (1959).
4. Tanford, C. & Reynolds, J. *Nature's Robots: A History of Proteins* Ch. 12 (Oxford Univ. Press, Oxford, 2001).
5. Tanford, C. How protein chemists learned about the hydrophobic factor. *Protein Sci.* **6**, 1358–1366 (1997).
6. Dix, S., Crain, J., Pooh, W. C. K., Finney, J. L. & Soper, A. K. Molecular segregation observed in a concentrated alcohol–water solution. *Nature* **416**, 829–832 (2002).
7. Swope, W. C. & Andersen, H. C. A molecular dynamics method for calculating the solubility of gases in liquids and the hydrophobic hydration of inert gas atoms in aqueous solution. *J. Phys. Chem.* **88**, 6548–6556 (1984).
8. Pratt, L. R. & Chandler, D. Theory of the hydrophobic effect. *J. Chem. Phys.* **67**, 3683–3704 (1977).
9. Pratt, L. R. & Chandler, D. Hydrophobic solvation of nonspherical solutes. *J. Chem. Phys.* **73**, 3430–3433 (1980).
10. Pratt, L. R. & Chandler, D. Hydrophobic interactions and osmotic second virial coefficients for methanol in water. *J. Solution Chem.* **9**, 1–17 (1980).
11. Chandler, D. *Introduction to Modern Statistical Mechanics* Ch. 3, 5–7 (Oxford Univ. Press, New York, 1987).
12. Barrat, J.-L. & Hansen, J.-P. *Basic Concepts for Simple and Complex Liquids* (Cambridge Univ. Press, Cambridge, 2003).
13. Sharp, K. A., Nicholls, A., Fine, R. & Honig, B. Reconciling the magnitude of the microscopic and macroscopic hydrophobic effects. *Science* **252**, 106–109 (1991).
14. Ashbaugh, H. S., Kaler, E. W. & Paulaitis, M. E. A "Universal" surface area correlation for molecular hydrophobic phenomena. *J. Am. Chem. Soc.* **121**, 9243–9244 (1999).
15. Tanford, C. Interfacial free energy and the hydrophobic effect. *Proc. Natl Acad. Sci. USA* **76**, 4175–4176 (1979).
16. Bowron, D. T., Filippini, A., Roberts, M. A. & Finney, J. L. Hydrophobic hydration and the formation of a clathrate hydrate. *Phys. Rev. Lett.* **81**, 4164–4167 (1998).
17. Stillinger, F. H. Structure in aqueous solutions of nonpolar solutes from the standpoint of scaled-particle theory. *J. Solution Chem.* **2**, 141–158 (1973).
18. Dill, K. A. & Bromberg, S. *Molecular Driving Forces* Ch. 16, 30 (Garland Science, New York, 2003).
19. Murphy, K. P. Hydration and convergence temperatures: on the use and interpretation of correlation plots. *Biophys. Chem.* **51**, 311–326 (1994).
20. Lum, K., Chandler, D. & Weeks, J. D. Hydrophobicity at small and large length scales. *J. Phys. Chem. B* **103**, 4570–4577 (1999).
21. Huang, D. M. & Chandler, D. The hydrophobic effect and the influence of solute–solvent attractions. *J. Phys. Chem. B* **106**, 2047–2053 (2002).
22. Wallqvist, A. & Berne, B. J. Computer simulation of hydrophobic hydration forces on stacked plates at short range. *J. Phys. Chem.* **99**, 2893–2899 (1995).
23. Gerstein, M. & Lynden-Bell, R. M. Simulation of water around a model protein helix. 1. Two-dimensional projections of solvent structure. *J. Phys. Chem.* **97**, 2982–2990 (1993).
24. Ashbaugh, H. S. & Paulaitis, M. E. Effect of solute size and solute–water attractive interactions on hydration water structure around hydrophobic solutes. *J. Am. Chem. Soc.* **123**, 10721–10728 (2001).
25. Huang, D. M., Geissler, P. L. & Chandler, D. Scaling of hydrophobic free energies. *J. Phys. Chem. B* **105**, 6704–6709 (2001).
26. Lee, C. Y., McCammon, J. A. & Rossky, P. J. The structure of liquid water at an extended hydrophobic surface. *J. Chem. Phys.* **80**, 4448–4455 (1984).
27. Rowlinson, J. S. & Widom, B. *Molecular Theory of Capillarity* Ch. 8 (Oxford Univ. Press, Oxford, 1982).
28. Smith, R. & Tanford, C. Hydrophobicity of long chain n-alkyl carboxylic acids, as measured by their distribution between heptane and aqueous solutions. *Proc. Natl Acad. Sci. USA* **70**, 289–293 (1973).
29. Tanford, C. *The Hydrophobic Effect: Formation of Micelles & Biological Membranes* Ch. 1–4, 8 (Wiley, New York, 1980).
30. Raschke, T. M., Tsai, J. & Levitt, M. Quantification of the hydrophobic interaction by simulations of the aggregation of small hydrophobic solutes in water. *Proc. Natl Acad. Sci. USA* **98**, 5965–5969 (2001).

31. Ten Wolde, P. R. & Chandler, D. Drying induced hydrophobic polymer collapse. *Proc. Natl Acad. Sci. USA* **99**, 6539–6543 (2002).
32. Chandler, D., Weeks, J. D. & Andersen, H. C. The van der Waals picture of liquids, solids and phase transformations. *Science* **220**, 787–794 (1983).
33. Scatena, L. F. & Richmond, G. L. Orientation, hydrogen bonding, and penetration of water at the organic/water interface. *J. Phys. Chem.* **B105**, 11240–11250 (2001).
34. Ball, P. Chemical physics: how to keep dry in water. *Nature* **423**, 25–26 (2003).
35. Jensen, T. R. et al. Water in contact with extended hydrophobic surfaces: Direct evidence of weak dewetting. *Phys. Rev. Lett.* **90**, 086101–086104 (2003).
36. Zhang, X., Zhu, Y. & Granick, S. Hydrophobicity at a Janus interface. *Science* **295**, 663–666 (2002).
37. Larson, R. G. *Structure and Rheology of Complex Fluids* Ch. 12 (Oxford Univ. Press, New York, 1999).
38. Maibaum, L., Dinner, A. R. & Chandler, D. Micelle formation and the hydrophobic effect. *J. Phys. Chem.* **B108**, 6778–6781 (2004).
39. Finney, J. L. Water? What's so special about it? *Phil. Trans. R. Soc. Lond. B* **359**, 1145–1165 (2004).
40. Tanford, C. *Ben Franklin Still the Waves* Ch. 14 (Oxford Univ. Press, Oxford, 2004).
41. Huang, D. M. & Chandler, D. Cavity formation and the drying transition in a Lennard-Jones fluid. *Phys. Rev. E* **61**, 1501–1506 (2000).
42. Bolhuis, P. G. & Chandler, D. Transition path sampling of cavitation between molecular scale solvophobic surfaces. *J. Chem. Phys.* **113**, 8154–8160 (2000).
43. Weeks, J. D. Connecting local structure to interface formation: A molecular scale van der Waals theory of non-uniform liquids. *Annu. Rev. Phys. Chem.* **53**, 533–562 (2002).
44. Southall, N. T. & Dill, K. A. The mechanism of hydrophobic solvation depends on solute radius. *J. Phys. Chem. B* **104**, 1326–1331 (2003).
45. Binder, K., Landau, D. P. & Ferrenberg, A. M. Wetting and capillary condensation of lattice gases in thin film geometry. *Ber. Bunsenges. Phys. Chem.* **98**, 340–345 (1994).
46. Maibaum, L. & Chandler, D. A coarse-grained model of water confined in a hydrophobic tube. *J. Phys. Chem. B* **107**, 1189–1193 (2003).
47. Smit, B. et al. Computer simulations of a water/oil interface in the presence of micelles. *Nature* **348**, 624–625 (1990).
48. Wu, D., Chandler, D. & Smit, B. Electrostatic analogy for surfactant assemblies. *J. Phys. Chem.* **96**, 4077–4083 (1992).
49. Larson, R. G. Monte Carlo simulation of microstructural transitions in surfactant systems. *J. Chem. Phys.* **96**, 7904–7918 (1992).
50. Garde, S., Hummer, G., Garcia, A. E., Paulaitis, M. E. & Pratt, L. R. Origin of entropy convergence in hydrophobic hydration and protein folding. *Phys. Rev. Lett.* **77**, 4966–4968 (1998).
51. Murphy, K. P., Privalov, P. L. & Gill, S. J. Common features of protein unfolding and dissolution of hydrophobic compounds. *Science* **247**, 559–561 (1990).
52. Huang, D. & Chandler, D. Temperature and length scale dependence of hydrophobic effects and their possible implications for protein folding. *Proc. Natl Acad. Sci. USA* **97**, 8324–8327 (2000).
53. Baldwin, R. L. Temperature dependence of the hydrophobic interaction in protein folding. *Proc. Natl Acad. Sci. USA* **83**, 8069–8072 (1986).
54. Gerstein, M. & Chothia, C. Packing at the protein-water interface. *Proc. Natl Acad. Sci. USA* **93**, 10167–10172 (1996).
55. Levy, Y. & Onuchic, J. N. Water and proteins: A love-hate relationship. *Proc. Natl Acad. Sci. USA* **101**, 3325–3326 (2004).
56. Rabani, E., Reichman, D. R., Geissler, P. L. & Brus, L. E. Drying-mediated self-assembly of nanoparticles. *Nature* **426**, 271–274 (2003).
57. Lum, K. & Chandler, D. Phase diagram and free energies of vapor films and tubes for a confined fluid. *Int. J. Thermophys.* **19**, 845–855 (1998).
58. Parker, J. L., Claesson, P. M. & Attard, P. Bubbles, cavities, and the long-ranged attraction between hydrophobic surfaces. *J. Phys. Chem.* **98**, 8468–8480 (1994).
59. Frenkel, D. & Smit, B. *Understanding Molecular Simulation* 2nd edn Ch. 7 (Academic, San Diego, 2002).
60. Hummer, G., Garde, S., Garcia, A. E., Pohorille, A. & Pratt, L. R. An information theory model of hydrophobic interactions. *Proc. Natl Acad. Sci. USA* **93**, 8951–8955 (1996).
61. Morrison, T. J. & Billett, F. The salting-out of non-electrolytes. Part II. The effect of variation in non-electrolytes. *J. Chem. Soc.* **3819–3822** (1952).
62. Chandler, D. Gaussian field model of fluids with an application to polymeric fluids. *Phys. Rev. E* **48**, 2898–2905 (1993).
63. Silverstein, K. A. T., Haymet, A. D. J. & Dill, K. A. The strength of hydrogen bonds in liquid water and around nonpolar solutes. *J. Am. Chem. Soc.* **122**, 8037–8041 (2000).
64. Gallagher, K. R. & Sharp, K. A. A new angle on heat capacity changes in hydrophobic solvation. *J. Am. Chem. Soc.* **125**, 9853–9860 (2003).
65. Gallicchio, E., Kubo, M. M. & Levy, R. M. Enthalpy-entropy and cavity decomposition of alkane hydration free energies: numerical results and implications for theories of hydrophobic solvation. *J. Phys. Chem. B* **104**, 6271–6285 (2000).
66. Mackay, D. & Shiu, W. Y. A critical review of Henry's Law constants for chemicals of environmental interest. *J. Phys. Chem. Ref. Data* **10**, 1175–1199 (1981).
67. Ben-Naim, B. *Hydrophobic Interactions* Ch. 3 (Plenum, New York, 1980).
68. Mackay, D., Shiu, W. Y. & Ma, K. C. *Illustrated Handbook of Physical-Chemical Properties and Environmental Fate of Organic Chemicals* Vol. III, 117, 170 (CRC Press, Boca Raton, 1993).

Acknowledgements My research on hydrophobicity was supported by the National Science Foundation and the US Department of Energy. I thank L. Maibaum for discussions and help in writing this review. I am also indebted to R. Levy and C. Tanford for constructive criticisms of an earlier draft. My choices for references are illustrative, not comprehensive.

Author Information Reprints and permissions information is available at npg.nature.com/reprintsandpermissions. The author declares no competing financial interests. Correspondence should be addressed to D.C. (chandler@ccchem.berkeley.edu).